

## Natural Product Micheliolide (MCL) Irreversibly Activates Pyruvate Kinase M2 and Suppresses Leukemia

Jing Li, Shanshan Li, Jianshuang Guo, Qiuying Li, Jing Long, Cheng Ma, Yahui Ding, Chunli Yan, Liangwei Li, Zhigang Wu, He Zhu, Keqin Kathy LI, Liuqing Wen, Quan Zhang, Qingqing Xue, Caili Zhao, Ning Liu, Ivaylo Ivanov, Ming Luo, Rimo Xi, Haibo Long, Peng George Wang, and Yue Chen

*J. Med. Chem.*, **Just Accepted Manuscript** • DOI: 10.1021/acs.jmedchem.8b00241 • Publication Date (Web): 11 Apr 2018

Downloaded from <http://pubs.acs.org> on April 11, 2018

### Just Accepted

“Just Accepted” manuscripts have been peer-reviewed and accepted for publication. They are posted online prior to technical editing, formatting for publication and author proofing. The American Chemical Society provides “Just Accepted” as a service to the research community to expedite the dissemination of scientific material as soon as possible after acceptance. “Just Accepted” manuscripts appear in full in PDF format accompanied by an HTML abstract. “Just Accepted” manuscripts have been fully peer reviewed, but should not be considered the official version of record. They are citable by the Digital Object Identifier (DOI®). “Just Accepted” is an optional service offered to authors. Therefore, the “Just Accepted” Web site may not include all articles that will be published in the journal. After a manuscript is technically edited and formatted, it will be removed from the “Just Accepted” Web site and published as an ASAP article. Note that technical editing may introduce minor changes to the manuscript text and/or graphics which could affect content, and all legal disclaimers and ethical guidelines that apply to the journal pertain. ACS cannot be held responsible for errors or consequences arising from the use of information contained in these “Just Accepted” manuscripts.

# Natural Product Micheliolide (MCL) Irreversibly Activates Pyruvate Kinase M2 and Suppresses Leukemia

Jing Li,<sup>†</sup> Shanshan Li,<sup>‡</sup> Jianshuang Guo,<sup>†</sup> Qiuying Li,<sup>†</sup> Jing Long,<sup>†</sup> Cheng Ma,<sup>‡</sup> Yahui Ding,<sup>†</sup>  
Chunli Yan,<sup>‡</sup> Liangwei Li,<sup>‡</sup> Zhigang Wu,<sup>‡</sup> He Zhu,<sup>‡</sup> Keqin Kathy Li,<sup>‡</sup> Liuqing Wen,<sup>‡</sup> Quan  
Zhang,<sup>†</sup> Qingqing Xue,<sup>†</sup> Caili Zhao,<sup>†</sup> Ning Liu,<sup>†</sup> Ivaylo Ivanov,<sup>‡</sup> Ming Luo,<sup>‡</sup> Rimo Xi,<sup>†</sup> Haibo  
Long,<sup>§</sup> Peng George Wang,<sup>\*,†,‡</sup> Yue Chen<sup>\*,†</sup>

<sup>†</sup>State Key Laboratory of Medicinal Chemical Biology, College of Pharmacy and Tianjin Key  
Laboratory of Molecular Drug Research, Nankai University, Haihe Education Park, 38 Tongyan  
Road, Tianjin 300350, China. <sup>‡</sup>Center for Diagnostics and Therapeutics, Department of  
Chemistry, Georgia State University, Atlanta, GA 30303, USA. <sup>§</sup>Department of Nephrology,  
Zhujiang Hospital, Southern Medical University, Guangzhou, 510280, China.

**KEYWORDS:** micheliolide, pyruvate kinase, activator, leukemia

**ABSTRACT** Metabolic reprogramming of cancer cells is essential for tumorigenesis, in which  
pyruvate kinase M2 (PKM2), the low activity isoform of pyruvate kinase, plays a critical role.  
Herein, we describe the identification of a nature-product-derived micheliolide (MCL) that  
selectively activates PKM2 through the covalent binding at residue cysteine424 (C424), which is

1  
2  
3  
4  
5  
6 not contained in PKM1. This interaction promotes more tetramer formation, inhibits the  
7  
8 lysine433 (K433) acetylation, and influences the translocation of PKM2 into the nucleus. In  
9  
10 addition, the pro-drug dimethylaminomicheliolide (DMAMCL) with similar properties as MCL,  
11  
12 significantly suppresses the growth of leukemia cells and tumorigenesis in a zebrafish xenograft  
13  
14 model. Cell-based assay with knock down PKM2 expression verifies the effects of MCL are  
15  
16 dependent on PKM2 expression. DMAMCL is currently in clinical trials in Australia and shows  
17  
18 encouraging treatment results, our discovery may provide valuable pharmacological mechanism  
19  
20 for the clinical treatment and benefit the development of new anti-cancer agents.  
21  
22  
23  
24

## 25 INTRODUCTION

26  
27  
28 Metabolic reprogramming towards aerobic glycolysis is a critical hallmark of cancers,  
29  
30 enabling cancer cells to obtain more biosynthetic materials for the growth and division of rapidly  
31  
32 proliferating cells.<sup>1</sup> Pyruvate kinases, which catalyzes the conversion of phosphoenol-pyruvate  
33  
34 (PEP) to pyruvate at the final step of glycolysis, has been shown to be crucial in the regulation of  
35  
36 cancer metabolic reprogramming.<sup>2-3</sup> Multiple lines of evidence have indicated that the M2  
37  
38 isoform of pyruvate kinase (PKM2) is upregulated in most cancer cells and tumors tested so far.<sup>1</sup>  
39  
40 In contrast to its splice variant PKM1, which is expressed in normal differentiated tissues as a  
41  
42 stable tetramer, PKM2 exists in equilibrium among monomer, dimer, and tetramer forms, which  
43  
44 was regulated by the allosteric binding of metabolic effectors or posttranslational modifications  
45  
46 (**Figure 1A**).<sup>2,4</sup> These different catalytic and regulatory properties are all ascribe to 22 distinct  
47  
48 amino acids between PKM1 and PKM2 (**Figure 1B**).<sup>1</sup> In cancer cells, more negative allosteric  
49  
50 modulations, including phosphor-tyrosine and numerous post-translational modifications, cause  
51  
52 the PKM2 tetramer to dissociate into a dimeric formation. Dimeric PKM2 is much less active,  
53  
54  
55  
56  
57  
58  
59  
60

and its presence diverts the glycolytic flux to increased biomass production, contributing to oncogenesis.<sup>5-6</sup> In addition, dimeric PKM2 has the potential to translocate into the nucleus to act as transcriptional regulators of genes that promote tumorigenesis and migration.<sup>5-8</sup> Consequently, much effort has focused on the discovery and development of small-molecule PKM2 activators to promote tetramer formation or initiate its activity.<sup>9, 10</sup> Herein, we describe a novel natural-product-derived PKM2 activator that shows promising efficacy for leukemia treatment and has entered clinical trials.

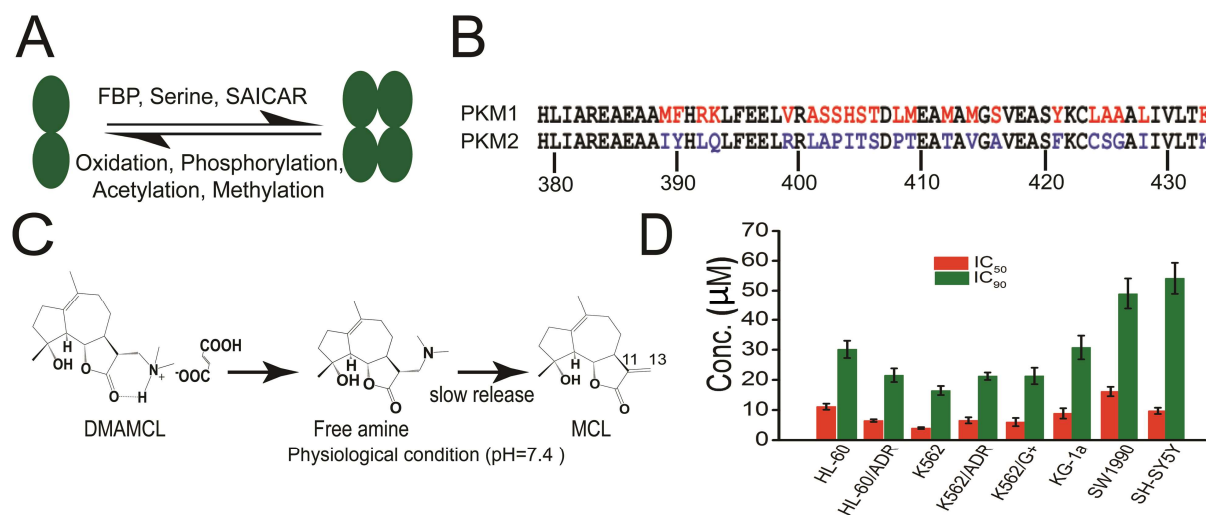


**Figure 1.** MCL is a novel allosteric activator of PKM2. (A), Allosteric regulations of PKM2. (B), Splice variant amino acids between PKM1 and PKM2. The 22 distinct amino acids are marked in red for PKM1 and in blue for PKM2. (C), the mechanism of sustainable release of MCL by DMAMCL under neutral conditions. (D), Inhibition profile of cancer cell lines by DMAMCL. Eight cancer cell lines were incubated with different concentrations of DMAMCL for 48 h. Cell proliferation was determined by MTT assay. Graphs depict mean  $\pm$  SEM from 6 independent experiments.

1  
2  
3  
4  
5  
6 Sesquiterpene lactones (SLs) are a class of natural products with varied biological and  
7  
8 pharmacological activities, including the common incorporation of trans- or cis-fused  $\gamma$ -lactone  
9  
10 containing an  $\alpha$ -methylene group.<sup>11</sup> Parthenolide (PTL), a SL isolated from feverfew (*Tanacetum*  
11  
12 *parthenium* L.) reportedly inhibits the proliferation of various human cancer cells *in vitro*.<sup>12, 13</sup>  
13  
14 However, PTL's lack of stability under both acidic and basic conditions, coupled with poor  
15  
16 solubility, has severely limited its medicinal applications.<sup>14</sup> In our previous work, we identified  
17  
18 micheliolide (MCL), a more stable guaianolide SL (GSL) (**Figure 1C**), as a new potent lead  
19  
20 compound for reducing the proportion of acute myelogenous leukemia (AML) cells and glioma  
21  
22 cells.<sup>15, 16</sup> Most strikingly, dimethylaminomicheliolide (DMAMCL, commercial name: ACT001),  
23  
24 the pro-drug of MCL, can release MCL slowly under physiological conditions<sup>16</sup> and was recently  
25  
26 approved for clinical trials in Australia (trial ID: ACTRN12616000228482). However, the  
27  
28 pharmacodynamic markers and cellular mechanism of DMAMCL remain unknown, making  
29  
30 their identification crucial for clinical treatment and designing more effective treatments.  
31  
32  
33  
34  
35

36 In this present work, we determined that MCL is a novel natural-product-derived, covalent,  
37  
38 and selective activator of PKM2 via binding to the conserved cysteine424 (C424) residue of  
39  
40 PKM2, but not PKM1. This binding induces the irreversible tetramerization of PKM2, which is  
41  
42 essential for high pyruvate kinase activity. Concomitantly, this allosteric regulation decreases  
43  
44 lysine433 (K433) acetylation of PKM2, and lowers PKM2 nucleus translocation, which is vital  
45  
46 for its non-metabolic function in cell proliferation and tumorigenesis. Combined with the  
47  
48 proliferation inhibition of several cancer cell lines and the repression of leukemia *in vivo*,  
49  
50 DMAMCL represents the first natural lead compound for the development of PKM2-targeted  
51  
52 therapeutic agents to enter clinical development.  
53  
54  
55  
56  
57  
58  
59  
60

## RESULTS AND DISCUSSION

### *Micheliolide derivative DMAMCL inhibits multiple cancer cells in vitro.*

Our previous work has demonstrated that MCL is a potent inhibitor of AML cells<sup>16</sup> and glioma cells.<sup>15</sup> To increase the bioavailability of MCL, we also synthesized the dimethylamino Michael adduct of MCL (DMAMCL),<sup>16</sup> which exhibited high stability, lower toxicity and sustainable release of MCL, under physiological or neutral conditions (**Figure 1C**). Here, a wide range of cancer cell lines, including drug-resistant and sensitive leukemia cell lines (HL-60, K562, and KG-1a), a human pancreatic adenocarcinoma cell line (SW1990), and a human neuroblastoma cell line (SH-SY5Y), were treated with DMAMCL, and assayed for the cell viability by MTT (3-[4,5-dimethylthiazol-2-yl]-2,5-diphenyl tetrazolium). Cell growth was inhibited in all treated cancer cell lines (IC<sub>50</sub>: 3.9–16.2 μM; IC<sub>90</sub>: 16.4–54.14 μM) in a concentration-dependent manner (**Figure 1D** and **Figure S1**). Consistent with our previous studies, the leukemia cell lines were found to be more sensitive to DMAMCL, with an IC<sub>50</sub> of less than 12 μM.<sup>16</sup>

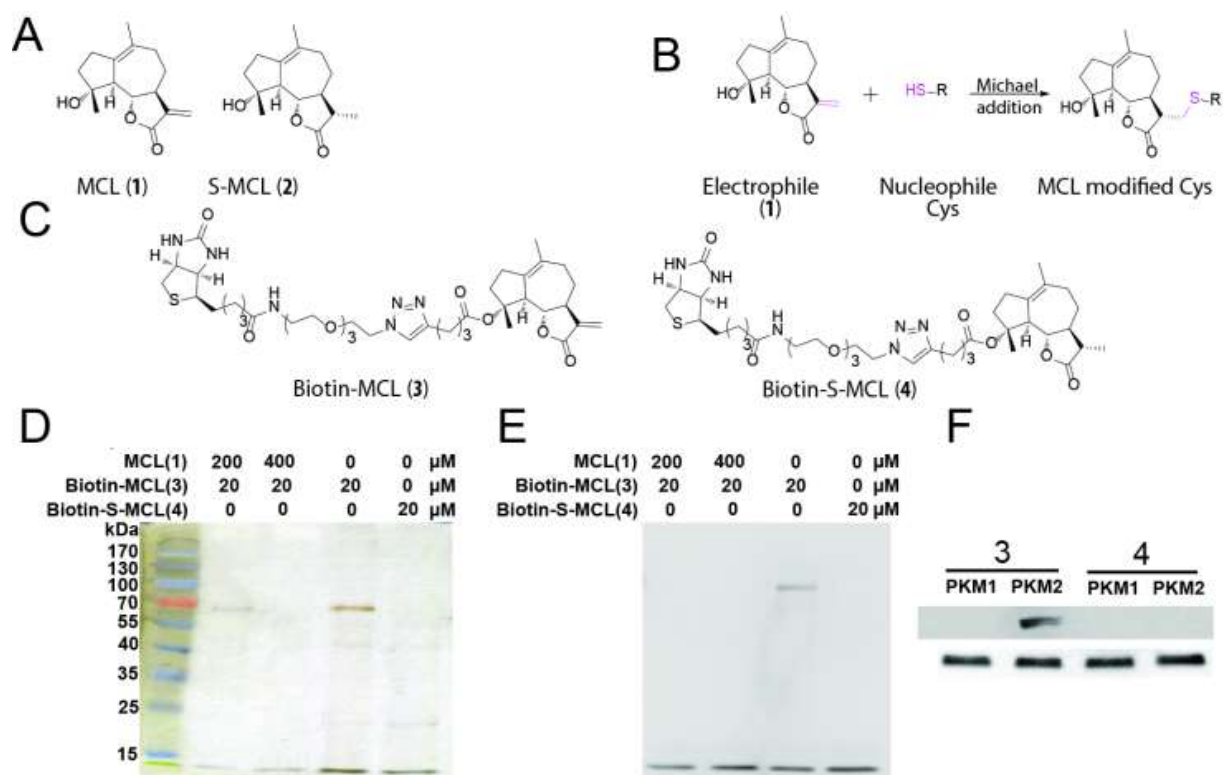


**Figure 2.** MCL directly binds to PKM2. (A), Structures of MCL (**1**, active) and S-MCL (**2**, inactive). (B), Michael addition mechanism of MCL and cysteine. (C), Structure of Biotin-MCL (**3**, active) and Biotin-S-MCL (**4**, inactive). (D), Silver staining of the pull-down fraction. HL60 cell lysates were incubated with **3** and **4** at 4°C overnight. For the treatment of **3**, a high concentration of MCL was added to the co-incubation. The lysates were used for streptavidin-agarose pull-down assays, and the precipitates were resolved by SDS-PAGE, followed by silver staining. (E), Western blot with the same sample as in silver staining but developed by anti-PKM2. (F), Western blot detection of the binding abilities of **3** and **4** with recombinant proteins PKM1 and PKM2, respectively. rPKM1 and rPKM2 were incubated with probe **3** or **4** at 4°C overnight. The mixture was then subjected to Western blot with streptavidin-HRP to detect the biotin-conjugated complex (top). The same sample was developed with anti-PKM1/PKM2

1  
2  
3  
4  
5  
6 antibody (bottom) to show the sample amount. All experiments were repeated at least three times,  
7  
8 with similar results.  
9

### 10 ***MCL specifically targets PKM2, not PKM1.***

11  
12  
13 To investigate the functional target of MCL (**1**) that is responsible for its anti-cancer activity,  
14  
15 we prepared biotin-conjugated probes for affinity purification. Our preliminary structure-activity  
16  
17 relationship (SAR) study revealed that when the 11,13-double bond of MCL was reduced to a  
18  
19 single bond to produce S-MCL (**2**) (**Figure 2A**), the inhibitory activity of MCL against leukemia  
20  
21 cells was completely abolished, even at a higher concentration (10  $\mu$ M).<sup>16</sup> These data indicate  
22  
23 that the 11,13-double bond of MCL (**1**) is crucial for its anti-cancer activity, most likely acting as  
24  
25 a reactive Michael acceptor and forming a covalent bond with the cysteine residues of its target  
26  
27 protein (**Figure 2B**). In contrast, MCL with slight modification to its C-region largely  
28  
29 maintained its activity against AML cells at a level comparable to that of MCL.<sup>16</sup> Thus, we  
30  
31 incorporated a biotin tag in the C-domain of MCL (**1**) and its inactive analogue S-MCL (**2**) to  
32  
33 yield a positive probe (**3**, Biotin-MCL) and a negative probe (**4**, Biotin-S-MCL) respectively  
34  
35 (**Figure 2C and Scheme S1**).  
36  
37  
38  
39

40  
41 Next, HL60 cell lysates were incubated with positive (**3**) and negative (**4**) probes, and the  
42  
43 mixtures were separately pulled down with streptavidin-coated agarose beads, followed by gel  
44  
45 electrophoresis and silver staining. A single band with a molecular mass of ~60 kDa was clearly  
46  
47 precipitated by **3** but not by **4** (**Figure 2D**). In addition, this band could be suppressed by a high  
48  
49 concentration of MCL. Peptide mass fingerprinting data analysis identified the MCL-bound  
50  
51 protein was PKM2 (**Figure S2**). Using immunoblotting, we also observed the presence of PKM2  
52  
53 in the precipitates (**Figure 2E**). To verify the selectivity of this binding, we expressed  
54  
55 recombinant PKM2 (rPKM2) and PKM1 (rPKM1) *in vitro* and incubated them with positive (**3**)  
56  
57  
58  
59  
60

and negative (4) probes respectively. The positive probe (3) effectively bound to rPKM2 but not rPKM1 (Figure 2F), further supporting the notion that PKM2, not PKM1, is the direct target of MCL.

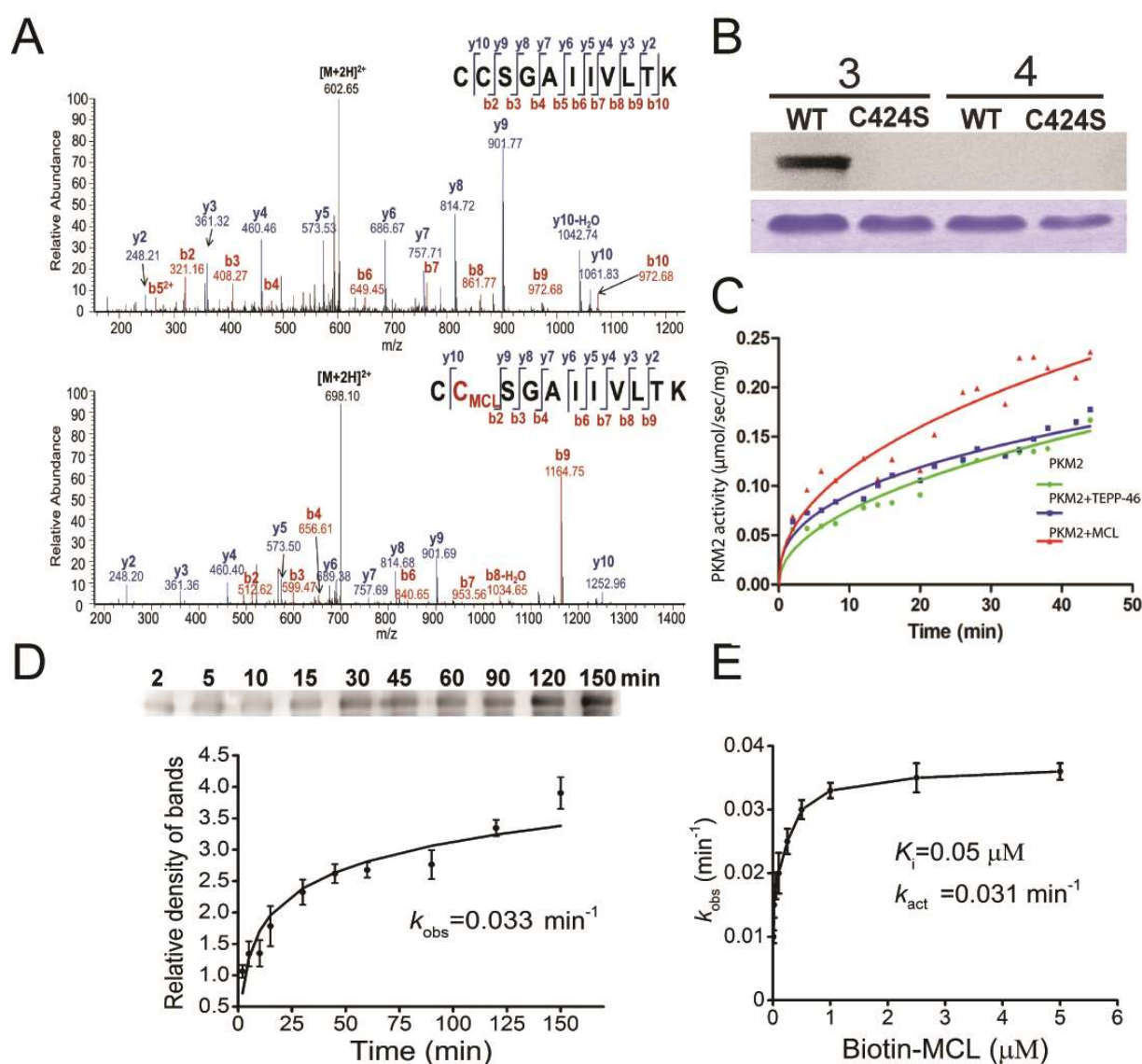


**Figure 3.** MCL targets C424 of PKM2 and activates its pyruvate kinase activity. (A), MS/MS analysis of the C424-containing tryptic peptide for rPKM2 incubated without (top) and with (bottom) MCL for 60 min at RT. C in red color represents the cysteine bound by MCL. (B),

1  
2  
3  
4  
5  
6 Recombinant WT PKM2 and its mutant (C424S) incubated with biotin-MCL for 60 min at RT,  
7  
8 followed by SDS-PAGE (bottom) and Western blot to detect biotin (top). (C), Recombinant  
9  
10 PKM2 proteins were incubated with MCL, TEPP-46 at 4  $\mu$ M for 50 min at RT, and their  
11  
12 pyruvate kinase activity was monitored over 40 min. (D), Determination of  $K_{obs}$  for the  
13  
14 interaction of PKM2 (0.25  $\mu$ M) with biotin-MCL (20  $\mu$ M) for different periods of time, as  
15  
16 described in the Supplementary Methods. (E), Plotting the  $K_{obs}$  values for the binding of PKM2  
17  
18 as a function of MCL at different concentrations.  
19  
20  
21

### 22 *C424 of PKM2 is critical for binding to MCL.*

23  
24

25  
26 The 11,13-double bond of MCL (**1**) is a reactive Michael acceptor, we speculated that some  
27  
28 conserved cysteine residues in PKM2 are the binding sites of MCL. To identify the specific  
29  
30 residues modified by MCL, we incubated the rPKM2 protein with or without MCL. After the  
31  
32 reaction, the rPKM2 protein was digested with trypsin and then analyzed by LC-MS/MS. The  
33  
34 mass of the Cys424-containing peptide CCSGAIIVLTK was measured as 1220.626 Da in the  
35  
36 absence of MCL and 1411.745 Da in the presence of MCL. The calculated mass shift of 191.120  
37  
38 Da is consistent with the addition of one molecular unit of MCL. MS/MS analyses of both  
39  
40 unmodified and modified C424-containing peptides provided a partial series of  $\gamma$ -ion fragments  
41  
42 corresponding to the peptide sequence. Both MS/MS spectra had the same mass from  $y_2$  to  $y_9$ ,  
43  
44 whereas the mass shifted by 191.120 Da for the C424-containing fragment (from  $y_{10}$ ) in the  
45  
46 spectra of the modified peptide (**Figure 3A**). Interestingly, C424 is located at the C-C interface  
47  
48 of two dimers, which can affect subunit interaction, enzymatic activity, or both.<sup>17</sup> To confirm  
49  
50 that C424 residue was the only modified site of MCL, rPKM2 and mutant rPKM2-C424S were  
51  
52 further expressed and incubated with biotin-MCL (**3**) or inactive biotin-MCL (**4**) and detected by  
53  
54 western blot. Contrast to rPKM2-C424, only rPKM2 incubated with biotin-MCL (**3**) produced a  
55  
56  
57  
58  
59  
60

1  
2  
3  
4  
5  
6 signal with anti-biotin, supporting our conclusion that MCL selectively binds to PKM2 at C424  
7  
8 site (**Figure 3B**).  
9

### 10 ***MCL activates the pyruvate kinase activity of PKM2.***

11  
12  
13 To determine the affect of MCL on PKM2 activity, we measured the pyruvate kinase activity  
14 of rPKM2 proteins in the presence or absence of MCL with TEPP-46 as positive control. The  
15 results demonstrated that MCL effectively promoted the pyruvate kinase activity of rPKM2 with  
16 half-maximum activating concentration ( $AC_{50}$ ) at 6 nM, which was better than TEPP-46 ( $AC_{50}$   
17 = 92 nM) (**Figure 3C; Figure S3**). The potent activation of MCL may be due to the covalent  
18 binding of MCL, which irreversibly activates PKM2 with cumulative effect. However, the action  
19 mode of TEPP-46 is reversible and dependent on the available of FBP.<sup>9</sup>  
20  
21  
22  
23  
24  
25  
26  
27  
28

29 To test if MCL binds to PKM2 through an irreversible covalent modification, we next  
30 assessed this binding at certain time points for several biotin-MCL concentrations. The profile of  
31 PKM2 binding with biotin-MCL at various concentrations revealed a time-dependent saturation  
32 (**Figure 3D**), consistent with an irreversible modification mechanism.<sup>18</sup> The data were fit to  
33 determine the observed rate constants for binding ( $K_{obs}$ ) at each concentration. Plotting the  $K_{obs}$   
34 values as a function of the biotin-MCL (**3**) concentration revealed a saturation curve (**Figure 3E**).  
35 These data support a two-step reaction for the activation of PKM2 by MCL (**1**) that involves the  
36 non-covalent reversible binding of PKM2 to biotin-MCL (initial binding step,  $K_i$ ), which places  
37 the moderately reactive electrophile of MCL (**1**) close to a specific nucleophile on the protein,  
38 followed by a second step that results in a specific covalent linkage ( $k_{act}$ ). Based on this model,  
39 the  $k_{act}$  value for PKM2 binding with biotin-MCL (**3**) was calculated to be 0.031 min<sup>-1</sup> (**Figure**  
40 **3E**), suggesting a high specific reactivity, and the  $K_i$  value was 0.05  $\mu$ M (**Figure 3E**), indicating  
41  
42  
43  
44  
45  
46  
47  
48  
49  
50  
51  
52  
53  
54  
55  
56  
57  
58  
59  
60

1  
2  
3  
4  
5  
6 a high affinity. Overall, the efficiency of the binding of MCL to PKM2 was high ( $k_{\text{act}} / K_i$   
7  $= 1.03 \times 10^4 \text{ M}^{-1} \text{ s}^{-1}$ ), demonstrating that MCL (**1**) is a potent irreversible activator of PKM2.  
8  
9

10  
11 ***MCL promotes increased tetramer formation of PKM2 in vitro or in cells.***  
12

13  
14 Tetrameric PKM2 is the only form with high pyruvate kinase activity, we next evaluated  
15 whether the activation of MCL is accompanied by the tetramerization of PKM2. Size-exclusion  
16 chromatography analysis and fraction detection by SDS-PAGE were performed on rPKM2 and  
17 MCL-treated rPKM2. Chromatography of rPKM2 indicated that rPKM2 contained a mixed  
18 population of configurations (i.e., monomers, dimers and tetramers), with a tendency to  
19 tetramerize at higher concentrations (**Figure S4A**). Thus, a low concentration of rPKM2 (0.3  
20 mg/mL), with a higher population of monomers, was used to detect the allosteric effect of MCL.  
21  
22 As expected, the incubation of rPKM2 with 10  $\mu\text{M}$  MCL resulted in a significant shift towards a  
23 tetrameric configuration (**Figure S4B, C**).  
24  
25  
26  
27  
28  
29  
30  
31  
32

33  
34 Large existing phosphotyrosine (pTyr) proteins in cancer cells can bind PKM2 and catalyze  
35 the release of FBP from the enzyme.<sup>19</sup> To verify the same promotion effect of MCL on  
36 endogenous PKM2, we cultured leukemia HL60 cells treated with DMSO, MCL, pervanadate (a  
37 tyrosine phosphatase inhibitor, which can increase the amount of pTyr proteins) and pervanadate  
38 combined with MCL. The cellular proteins including endogenous PKM2 were then extracted,  
39 normalized, and analyzed by the same chromatographic method. According to tetramer and  
40 monomer formation of PKM2, different fractions were collected and detected by western blot  
41 with anti-PKM2 antibody. Compared to DMSO treatment, PKM2 with only pervanadate  
42 treatment appeared primarily as a dimer. In contrast, MCL treatment increased tetramer  
43 formation of PKM2, regardless of the presence or absence of pTyr. These data indicate that MCL  
44  
45  
46  
47  
48  
49  
50  
51  
52  
53  
54  
55  
56  
57  
58  
59  
60

acts as a potent tetramer inducer of PKM2 and cannot be competed-out by pTyr, even after treating the cells with pervanadate (**Figure 4A**).

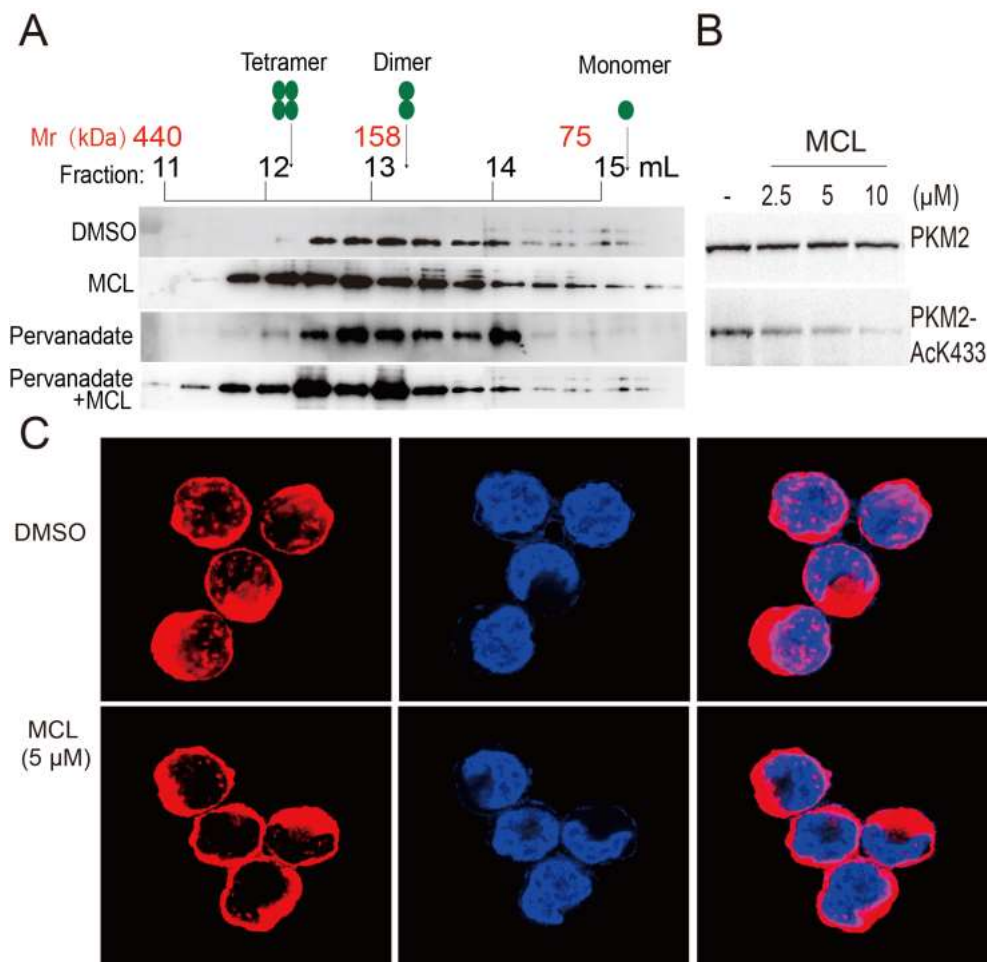


**Figure 4.** MCL promotes PKM2 tetramer formation and prevents AcK433 modification and nucleus translocation. (A), PKM2 subunit association was determined by western blot using anti-PKM2 (Cell signaling technology, 4053) of the chromatographic fractions of HL60 cells treated with MCL, pervanadate, and MCL combined pervanadate, lysed hypotonically and analyzed by size-exclusion chromatography. Mr, relative molecular weight. (B), Effect of MCL on the AcK433 of PKM2. HL60 cells were preincubated with MCL (0, 2.5, 5 and 10 μM) for 20h, followed by detection of endogenous PKM2 and AcK433 PKM2 by western blot. (C),

1  
2  
3  
4  
5  
6 Subcellular localization of total PKM2 and MCL treated PKM2 was examined by  
7 immunofluorescence microscopy in HL60 cells. HL60 cells were treated with MCL (5  $\mu$ M) or  
8 DMSO for 20 h and reacted with anti-PKM2. After overnight incubation, the second antibody  
9 Alexa Fluor 647 conjugated goat anti-rabbit IgG (red) for PKM2 and Hoechst 33342 (blue) for  
10 nucleus were added to image.  
11  
12  
13  
14  
15  
16  
17

18 ***MCL decreases the K433 acetylation of PKM2 and reduces its nuclear translocation.***  
19

20  
21 Recently, Lv et al. reported that upon the stimulation of mitogenic and oncogenic signals,  
22 PKM2 was acetylated by p300 acetyltransferase at lysine433 (K433), which inactivates PKM2 by  
23 interfering with FBP binding and promotes the nuclear accumulation.<sup>20</sup> Dimer PKM2, when  
24 located to the nucleus, can function as a protein kinase and transcriptional coactivator to trigger  
25 the expression of genes that promote tumorigenesis and migration.<sup>8, 20, 21</sup> To explore the  
26 intracellular effect of MCL on PKM2, we incubated HL60 leukemia cells with DMSO or MCL,  
27 then extracted the cellular protein to detect the AcK433 modification of PKM2. Western blot  
28 developed with anti-AcK433-PKM2 indicated that AcK433 decreased with MCL treatment in a  
29 dose-dependent manner (**Figure 4B**, bottom). Meanwhile, western blot developed with anti-  
30 PKM2 revealed that cellular PKM2 was present in comparable amounts among the different  
31 samples (**Figure 4B**, top). These data indicate that the MCL treatment has no effect on the protein  
32 level of PKM2, but reduces the acetylation at K433, contributing to the tetramerization of PKM2  
33 indirectly. Interestingly, immune-fluorescence analysis revealed that MCL treatment at 5  $\mu$ M  
34 (note: most cells died at 10  $\mu$ M, presumably as a result of nuclear damage) for 12 h resulted in  
35 retardation of the nuclear accumulation of PKM2 in HL60 cells (**Figure 4C**). Western blot  
36 analysis of sub-cellular fraction also confirmed the decrease of PKM2 in nuclear retardation  
37 (**Figure S5**). These results demonstrate that MCL is an effective PKM2 modulator, which  
38  
39  
40  
41  
42  
43  
44  
45  
46  
47  
48  
49  
50  
51  
52  
53  
54  
55  
56  
57  
58  
59  
60

inhibits both acetylation modification and nuclear translocation in cells, further suppresses the transcriptional regulation in tumorigenesis.

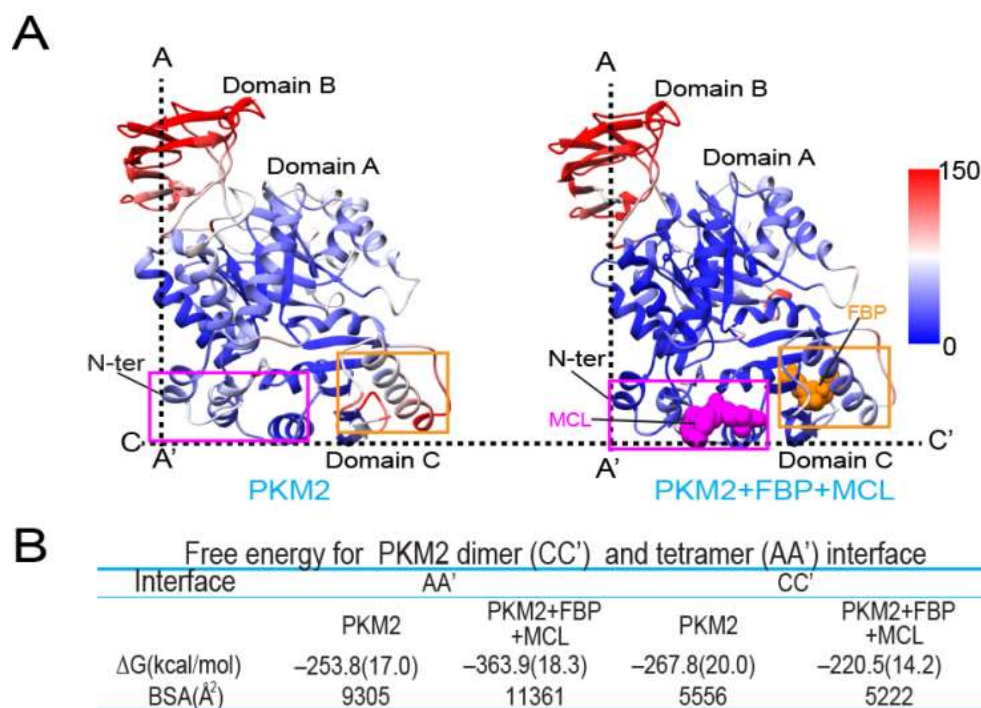


**Figure 5.** Activator MCL promotes PKM2 tetramer formation (PDB ID: 1ZJH and 1T5A, 1ZJH is the apo tetrameric PKM2 structure. 1T5A is the FBP bound tetrameric PKM2 structure). (A), Computed B-factors mapped onto the PKM2 models highlights conformational differences. Coloring corresponds to computed B-factor values from high (red) to low (blue). (B), Computed free energy of AA' and CC' interface. Per residue binding energies computed from the 1D MM/GBSA decomposition. Residues are colored according to the value of the binding energy in kcal/mol from red (positive) to blue (negative). The bound MCL are shown as magenta spheres. The large (AA') and small (CC') interfaces between monomers are presented as dashed lines. Only one monomer is shown.

### *Structural analysis of the binding mode between MCL and PKM2.*

1  
2  
3  
4  
5  
6 To better understand the structure and regulatory properties of MCL binding to PKM2, we  
7  
8 docked MCL into the human X-ray structure of PKM2 (PDB ID: 1T5A) using the docking  
9  
10 package GOLD 5.1.<sup>22</sup> Each PKM2 monomer is composed of four domains: the N-terminal, A-,  
11  
12 B- and C-domains (**Figure S6A, B, C**), and can form oligomeric assemblies (dimers, tetramers  
13  
14 and, to a lesser extent, higher order oligomers). In order to mimic covalent binding, we defined  
15  
16 two linking atoms, one from the MCL ligand (C13, **Figure 1C**) and the other from Cys424 (S),  
17  
18 and forced them to occupy the same steric volume.  
19  
20

21  
22 In the dimer formation, the subunit interface is formed by the adjacent C-domains (C-C' dimer  
23  
24 interface, **Figure S6A**). In the tetramer formation, an additional interface is introduced between  
25  
26 the neighboring A-domains (A-A' tetramer interface, **Figure S6A**). We firstly docked MCL  
27  
28 moiety among the A-, C- and N-terminal domains, and then performed extensive molecular  
29  
30 dynamics (MD) simulations and molecular mechanics/generalized Born surface area continuum  
31  
32 solvation (MM/GBSA) calculations to assess the stability of the tetramer or dimer with or  
33  
34 without MCL binding. The relative flexibilities of the MCL-bound and MCL-free complexes  
35  
36 were determined from the computed per residue B-factors. These values were calculated over the  
37  
38 last 40 ns of the MD trajectories, and subsequently mapped onto the PKM2 structures. Of the  
39  
40 four PKM2 domains (A-, B-, C- and N-terminus), the B-domain experienced larger fluctuations  
41  
42 during MD, while the A- and C- domains were less mobile, as these domains were involved in  
43  
44 dimer and tetramer formation (**Figure 5A**). Moreover, in the MCL-bound state, the A domain  
45  
46 exhibited considerably less flexibility, and the N-terminal domain induced tetramer formation,  
47  
48 which indicated that MCL binding can significantly stabilize the A-A' tetramer interface (**Figure**  
49  
50 **5A**). As for the interfacial binding energies of A-A' (tetramer formation) and C-C' (dimer  
51  
52 formation), C-C' binding energies were little fluctuated, but A-A' binding energies were greatly  
53  
54  
55  
56  
57  
58  
59  
60

1  
2  
3  
4  
5  
6 enhanced by the addition of MCL, and the binding free energy  $\Delta G_b$  increased from  $-253.8$   
7  $\text{kcal}\cdot\text{mol}^{-1}$  (PKM2) to  $-322.3 \text{ kcal}\cdot\text{mol}^{-1}$  (PKM2•MCL complex) (**Figure 5B**). To identify the  
8 structural features responsible for stabilizing the A-A' and C-C' interfaces, we decomposed  $\Delta G_b$   
9 into per residue contributions (1D MM/GBSA decomposition) Residue contributions were color  
10 mapped onto the structures of the respective interfaces (**Figure S6D, E**). In addition,  $\Delta G_{np}$  (or  
11 the buried surface area, BSA) correlated well with the overall binding energies, indicating that  
12 MCL promoted tetramer formation by increasing the BSA at the tetramer interface. Overall,  
13 these data suggest that new interactions at A-A' interface with MCL binding appear to be directly  
14 responsible for the observed increase in binding free energy and stabilization of the PKM2  
15 tetramers. In contrast, TEPP-46 was found in the A-A' interface and interacts with the  
16 surrounding residues Asp354, Ala388, Tyr390 and Leu394 through polar and van der Waals  
17 interactions. The binding residues and interaction energy of TEPP-46 are quite different from  
18 that of MCL.  
19  
20  
21  
22  
23  
24  
25  
26  
27  
28  
29  
30  
31  
32  
33  
34  
35  
36  
37  
38  
39  
40  
41  
42  
43  
44  
45  
46  
47  
48  
49  
50  
51  
52  
53  
54  
55  
56  
57  
58  
59  
60

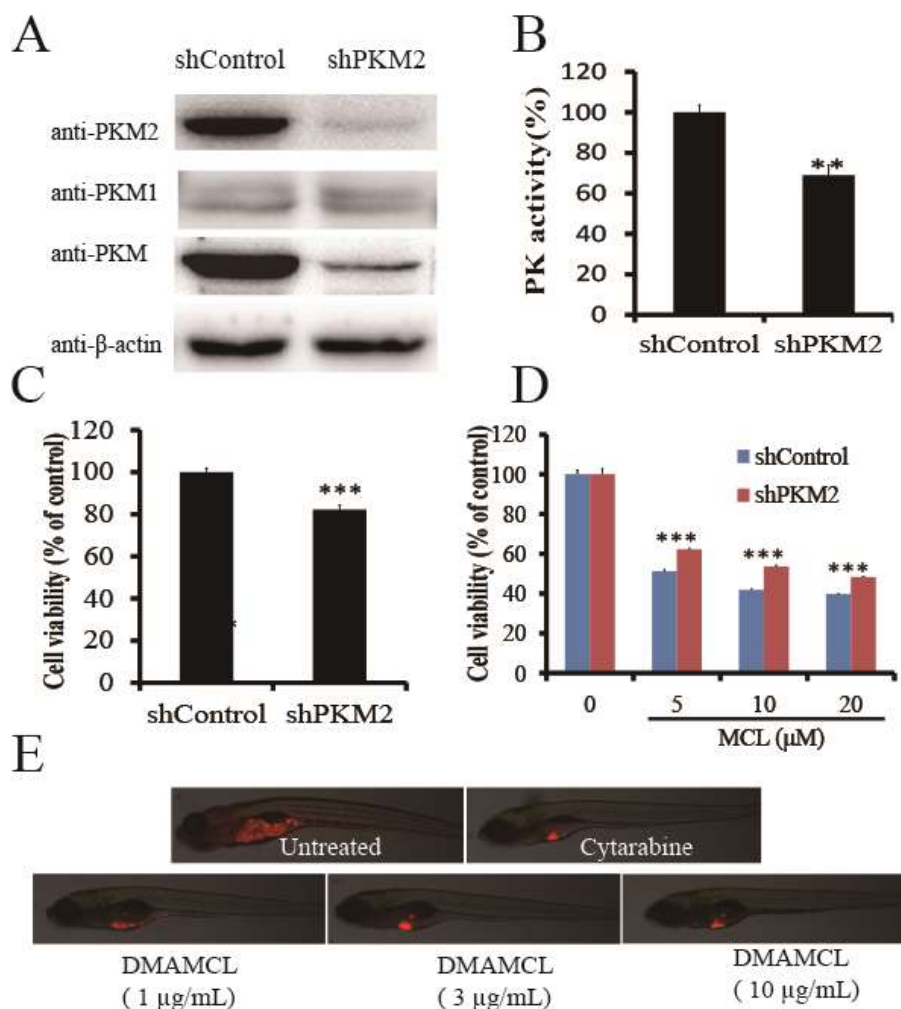


**Figure 6.** The anticancer effects of DMAMCL are dependent on PKM2. (A), Western blot detection of the expression of PKM1, PKM2 and PKM in the absence of endogenous PKM2, which was knocked down with short hairpin RNA. (B), Cell-based detection of pyruvate activity of HL60 cells with *shPKM2* and *shControl*. (C), Cell viability detection of pyruvate activity of HL60 cells with *shPKM2* and *shControl*. (D), PKM2 depletion desensitizes cancer cells to MCL treatment. (E), Representative fluorescent images of HL60 cell xenografted zebrafishes with treatment of DMAMCL, cytarabine or negative control. Approximately 300 HL60 cells were injected into the yolk sac of embryos. After injections, xenografted embryos were treated with a

1  
2  
3  
4  
5  
6 series of doses of DMAMCL (1, 3, 10  $\mu\text{g}/\text{mL}$ ), cytarabine at 200  $\mu\text{g}/\text{mL}$  as a positive drug  
7  
8 control, and saline as a negative control. After 3 days incubation, the number of embryos  
9  
10 exhibiting cancer cell dissemination was counted by microscopic observation (15 larvae / group).  
11  
12 Data represent the average  $\pm$  SD of three independent assays. \* =  $P < 0.05$ . \*\* =  $P < 0.01$ .  
13  
14

### 15 16 ***Anticancer activity of MCL is dependent on the expression of PKM2.***

17  
18 To investigate the influence of PKM2 on the MCL-mediated inhibition of leukemia cell  
19  
20 viability, we knock down the expression of PKM2 in HL60 cells by lentiviral delivery of specific  
21  
22 short hairpin RNA for PKM2 (*shPKM2*) or mock (*shControl*). Western blot showed that *shPKM2*  
23  
24 inhibited the expression of PKM2 but not PKM1 (**Figure 6A**), indicating the specificity of  
25  
26 *shPKM2*. Concomitantly, stable knockdown of PKM2 resulted in decreased pyruvate kinase  
27  
28 activity of PKM2 (69% of *shControl*) and reduced cell viability (83% of *shControl*) (**Figure 6B,**  
29  
30 **C**). These data were consistent to the results of Goldberg et al., in which cell viability was  
31  
32 drastically reduced among 10 cancer cell lines with the treatment of *shPKM2*.<sup>23</sup> Then *shPKM2*  
33  
34 and *shControl* cells were treated with MCL or DMSO for 24 h and assayed the cell viability.  
35  
36 Results indicate that the *shPKM2* cells are less sensitive to the inhibitory effect of MCL than  
37  
38 *shControl* cells (**Figure 6D**), implying the effect of MCL on cancer cell viability is mainly  
39  
40 dependent on PKM2.  
41  
42  
43  
44

### 45 46 ***Evaluation of the inhibitive effect of DMAMCL in xenograft zebrafish.***

47  
48 To assess the anti-cancer effects of DMAMCL, xenograft zebrafishes were established via  
49  
50 injection of human leukemia HL60 cells in zebrafish embryos. HL60 cells were first stained with  
51  
52 cell tracker CM-Dil (red fluorescence color) and then transplanted into zebrafish embryos at 2  
53  
54 days post fertilization (2dpf). Following transplantation, nine injected zebrafish groups were  
55  
56 treated with drugs at different dosages over the course of 3 days. Compared with the control  
57  
58  
59  
60

1  
2  
3  
4  
5  
6 group, 80% zebrafish died when the dosage of DMAMCL exceeded 20  $\mu\text{g/mL}$ , whereas the  
7  
8 survival rate approached 100% at a concentration of 10  $\mu\text{g/mL}$  or lower. Notably, with dosages  
9  
10 between 1–10  $\mu\text{g/mL}$ , DMAMCL produced a dose-dependent decrease in cell dissemination  
11  
12 (**Figure 6E**) with respect to both proliferation and migration. Results of this study indicated that  
13  
14 optimal inhibition of dissemination was observed with DMAMCL treatment at a dose of 10  
15  
16  $\mu\text{g/mL}$ , with proliferation and migration inhibition rates of 56.44% ( $P < 0.01$ ) and 58.10%  
17  
18 ( $P < 0.01$ ), which exceeded rates following cytarabine treatment (200  $\mu\text{g/mL}$ ) of 43.28% ( $P < 0.01$ )  
19  
20 and 44.04% ( $P < 0.01$ ) (**Table S1 and Table S2**).

21  
22  
23  
24 These data demonstrate that the activation of PKM2 by MCL results in significant suppression  
25  
26 of tumor growth *in vivo*, indicating DMAMCL acts as a novel PKM2 activator with promising  
27  
28 potential for anticancer therapeutics.  
29

## 30 31 CONCLUSIONS

32  
33 Targeting tumor-specific metabolic pathways is a novel strategy for cancer therapy.<sup>1</sup> Recent  
34  
35 studies have identified that PKM2 is abundantly expressed in AML cell lines and primary AML  
36  
37 patient samples.<sup>24-26</sup> Combined with the up-regulation in other cancer cells, PKM2 has been  
38  
39 identified as a promising potential target for cancer therapy.<sup>3</sup> However, PKM2 knockdown in  
40  
41 HCT116 and RKO colon cancer cells demonstrated that the growth of xenograft tumors is  
42  
43 unaffected *in vivo*.<sup>27</sup> Moreover, PKM2 knockdown accelerates tumor formation in a Breal-loss-  
44  
45 driven mice model of breast cancer.<sup>5</sup> In contrast, the genetic replacement of PKM2 with active  
46  
47 PKM1 decreased the proliferation of cancer cells *in vitro* and suppressed the formation of cancer  
48  
49 cell xenograft tumors in mice.<sup>1,9</sup> Thus, low pyruvate activity caused by inactive state of PKM2  
50  
51 (dimer) is the key for the proliferation of cancer cells within tumors.<sup>5</sup> Fixation PKM2 in its  
52  
53 active tetrameric form by activators is anticipated to be a novel treatment for cancer therapy.<sup>3,9,10</sup>  
54  
55  
56  
57  
58  
59  
60

1  
2  
3  
4  
5  
6 MCL, a natural guaianolide sesquiterpene lactone which discovered in *Michelia compressa*  
7  
8 and *Michelia champaca* plants, has been shown to exert potent anti-cancer properties on AML  
9  
10 and glioma cells.<sup>15, 16</sup> The present study demonstrated that DMAMCL inhibited several cancer  
11  
12 cells growth *in vitro*, and repressed tumor growth in leukemia HL60 xenografted zebrafish. To  
13  
14 determine the specific target of MCL, we analyzed the SAR of MCL and synthesized both a  
15  
16 positive (**3**) and negative (**4**) probe. Using this pair of probes, we found that MCL selectively  
17  
18 targeted PKM2 but not PKM1 in HL-60 cells. Through LC-MS/MS analysis and a PKM2  
19  
20 activity assay, we found that MCL selectively binds to the conserved C424 residue of PKM2,  
21  
22 promoting tetramer formation, and elevating pyruvate activity. These promising results indicate  
23  
24 that activation of PKM2 via natural product compound might be a useful anticancer strategy in  
25  
26 the clinic.  
27  
28  
29

30  
31 Interestingly, recent advances reported that various stimuli and post-translational  
32  
33 modifications can trigger PKM2 translocation into nucleus.<sup>17, 20, 28, 29</sup> Once accumulation in  
34  
35 nucleus, PKM2 functions as co-activator or protein kinase to promote tumor growth or  
36  
37 proliferation.<sup>7, 8, 21, 30, 31</sup> In this study, we found that MCL inhibited the K433 acetylation of  
38  
39 PKM2 but not the protein level. Meanwhile, the nuclear PKM2 was reduced concomitantly,  
40  
41 which will block its signaling role for proliferation. To our knowledge, MCL is the first known  
42  
43 or reported covalently-bound, natural-product-derived PKM2 modulator, which interfere the role  
44  
45 of PKM2 both in cytoplasm and nucleus.  
46  
47

48  
49 PKM2 integrates metabolic inputs and nuclear signaling in tumorigenesis, and has been  
50  
51 investigated as a novel target for cancer therapy. Data reported in this study argue that MCL, the  
52  
53 active drug derived from DMAMCL, enhances PKM2 activity by stably promoting the more  
54  
55  
56  
57  
58  
59  
60

1  
2  
3  
4  
5  
6 active tetrameric formation and reduces its nuclear translocation, which will unveil the  
7  
8 mechanism of DMAMCL and inform clinical trials for cancer treatment.  
9

## 10 **EXPERIMENTAL SECTION**

### 11 *Reagents and General Synthetic Procedures.*

12  
13  
14  
15 Reagents were purchased at the highest commercial quality and used without further  
16  
17 purification, unless otherwise stated. NMR spectra were recorded with a 400 MHz (<sup>1</sup>H: 400 MHz;  
18  
19 <sup>13</sup>C: 100 MHz) spectrometer and referenced to the solvent peak for CDCl<sub>3</sub>. Synthesis and  
20  
21 chemical confirmation of micheliolide (MCL), S-MCL, DMAMCL, biotin-S-MCL and biotin-  
22  
23 MCL are described in **SI Materials and Methods**. The purity of these compounds was  
24  
25 confirmed to be ≥95% by analytical HPLC with an ODS-C18 column (4.6 × 150 mm, 5 μm)  
26  
27 eluted at 1 mL/min with Milli-Q water and CH<sub>3</sub>CN. Antibodies and other reagents used in this  
28  
29 study were purchased directly from the vendors listed in **SI Materials and Methods**.  
30  
31

### 32 *Cell lines and culture.*

33  
34  
35 HL-60, KG-1a, K562, HL-60/ADR, KG-1a/ADR, K562/ADR, SW1990, SH-SY5Y were  
36  
37 purchased from ATCC and authenticated by short tandem repeat testing. All the cell lines were  
38  
39 maintained in appropriate medium as the manufacturer suggested. HL-60, KG-1a, K562, HL-  
40  
41 60/ADR, KG-1a/ADR, K562/ADR were cultured in RPMI 1640 medium (Sigma-Aldrich, St.  
42  
43 Louis, MO, USA) supplemented with 12% fetal bovine serum (FBS; Gibco BRL, Gaithersburg,  
44  
45 ML, USA), penicillin (100 IU/mL) and streptomycin (100 μg/mL) in a humidified incubator at  
46  
47 37°C and 5% CO<sub>2</sub> / 95% air. Prior to each experiment, HL-60/ADR, KG-1a/ADR, K562/ADR  
48  
49 cells were treated with 1 μmol/ml ADR (Sigma-Aldrich, St. Louis, MO, USA) for 10–28 days  
50  
51 and then cultured for 10 days without ADR exposure. SW1990, SH-SY5Y were cultured in  
52  
53 DMEM medium (Sigma-Aldrich, St. Louis, MO, USA) supplemented with 10% fetal bovine  
54  
55  
56  
57  
58  
59  
60

1  
2  
3  
4  
5  
6 serum (FBS; Gibco BRL, Gaithersburg, ML, USA), penicillin (100 IU/mL) and streptomycin  
7  
8 (100 µg/mL). All the cell lines were tested for mycoplasma contamination and were found to be  
9  
10 negative.

11  
12 For experiments, cells were treated with compounds for different concentrations with 0.1%  
13 dimethyl sulfoxide (DMSO; Sigma-Aldrich, St. Louis, MO, USA) as solvent control. Where  
14  
15 indicated, 100 µM pervanadate was added 10 min before cell lysis.  
16  
17

### 18 19 ***Plasmids, shRNA virus production, and infection.***

20  
21 Expression plasmids for human PKM1 and PKM2, pET28a-PKM1 and pET28a-PKM2  
22 plasmids were donated by Dr. Zhiren Liu's group. To get cysteine424 mutated PKM2 plasmid,  
23 site-directed mutant was constructed using QuikChange II XL Site-Directed Mutagenesis Kit  
24 (Stratagene, USA) and primers (Forward: 5'-attatggccccactg gagcacttgaaggagg-3'; Reverse: 5'-  
25 cctccttcaagtgtccagtgggg ccataat -3'). After confirming a 100% identities match by DNA  
26 sequencing (Invitrogen, Shanghai, China), the *E. coli* strain BL21 was transformed with  
27 constructs for next step of proteins purification.  
28  
29

30  
31 The shRNAs targeting the sequence of human *PKM2* (corresponding to exon 10 of the human  
32 PKM) and corresponding negative control (NC) were designed as previous reported.<sup>23</sup> The  
33 shRNA for *PKM2* was 5'-CCATAATCGTCCT CACCAA-3'; the shRNA for negative control  
34 was 5'-CUUACGCUGAGUACUUCGA-3'. The recombinant lentivirus containing *shPKM2* or  
35 *shControl* was packaged using hU6-MCS-Ubiquitin-EGFP-IRES-puromycin lenti-viral vector  
36 provided by Shanghai GeneChem (China). HL60 was infected by adding the lentiviral particles  
37 to the culture with 5 µg/mL polybrene. For generating stable cell lines, infected cells were  
38 selected with 1 µg/mL puromycin (Sigma) for 72 h.  
39  
40  
41  
42  
43  
44  
45  
46  
47  
48  
49  
50  
51  
52  
53  
54

### 55 ***Cell-based pyruvate kinase activity assay.***

56  
57  
58  
59  
60

1  
2  
3  
4  
5  
6 HL60 or HL60-shPKM2 leukemia cells were plated at  $2 \times 10^5$  cells per well (6-well plate) in  
7  
8 RPMI 1640 media plus 12% FBS. 100  $\mu$ M pervanadate was added 10 minutes prior to cell lysis.

9  
10 <sup>9</sup> Then, cells were lysed on ice with NP-40 buffer containing 2 mM DTT and protease inhibitors  
11  
12 about 30 minutes and clarified by centrifugation at 14,000 g for 5 minutes. The PK activity in  
13  
14 lysates was determined by Pyruvate Kinase Activity Assay (Sigma, MAK072-1KT).<sup>32</sup>

### 15 16 17 ***In vivo tumor models.***

18  
19 All animal studies were conducted according to protocols approved by the Animal Ethics  
20  
21 Committee of Nankai University, in accordance with ‘Principles of Laboratory Animal Care and  
22  
23 Use Programs’. Zebrafish (albino) were obtained from the Zebrafish International Resource  
24  
25 Center (Eugene, Oregon, USA) and housed in an automated fish housing system (Hunter  
26  
27 Biotechnology Inc, China) at 28°C. Care and treatment of zebrafish were conducted in  
28  
29 accordance with guidelines approved by the Association for Assessment and Accreditation of  
30  
31 Laboratory Animal Care (AAALAC).

### 32 33 34 35 ***Statistical analysis.***

36  
37 Kaplan-Meier survival analysis (SPSS 10.0; SPSS, Inc.) was used to compare drug-treated  
38  
39 versus control animals. An unpaired Student’s t-test was used to evaluate the difference between  
40  
41 two different treatments, where a P-value of less than 0.05 was considered statistically significant.  
42  
43 Statistical analyses were performed using PRISM software (Irvine, CA, USA).

## 44 45 46 47 **SUPPORTING INFORMATION**

48  
49 Supplementary figures and table, methods for chemical synthesis, MTT assay for DMAMCL,  
50  
51 pull-down of biotin-MCL bound proteins, molecular modeling, western blot, Immunofluore-  
52  
53 scence analysis, preparation of recombinant proteins, gel filtration of cell fraction, recombinant  
54  
55 PKM2 activity assay, protein identification by LC/MS/MS, kinetic determination of PKM2-MCL  
56  
57  
58  
59  
60

1  
2  
3  
4  
5  
6 interaction, and anti-cancer evaluation in HL60 cells xenografted zebrafish. These materials are  
7  
8 available free of charge *via* the Internet at <http://pubs.acs.org>.  
9

10  
11 **Molecular formula strings (CSV).**  
12

13  
14 **PDB ID CODES.**  
15

16  
17 Docked model of **1** into the FBP bound tetrameric PKM2 structure (PDB ID: 1T5A) and apo  
18 tetrameric PKM2 structure (PDB ID: 1ZJH) were shown in **Figure 5** and **Figure S5**. Authors  
19 will release the atomic coordinates upon article publication.  
20  
21  
22  
23

24  
25 **ABBREVIATIONS**  
26

27 MCL, micheliolide; S-MCL, single bond MCL; Biotin-MCL, biotin conjugated micheliolide;  
28 Biotin-S-MCL, biotin conjugated single bond micheliolide; PKM2, pyruvate kinase M2; PKM1,  
29 pyruvate kinase M1; PEP, phosphoenol-pyruvate; SLs, sesquiterpene lactones; PTL, parthenolide;  
30 GSL, guaianolide sesquiterpene lactone; AML, acute myelogenous leukemia; DMAMCL,  
31 dimethylaminomicheliolide; MTT, 3-[4,5-dimethylthiazol-2-yl]-2,5-diphenyl tetrazo- lium; SAR,  
32 structure-activity relationship; rPKM1, recombinant PKM1; rPKM2, recombinant PKM2; AC<sub>50</sub>,  
33 half-maximum activating concentration; pTyr, phosphotyrosine; MD, molecular dynamics;  $K_{obs}$ ,  
34 the observed rate constants for binding;  $K_i$ , the apparent dissociation constant for the initial  
35 PKM2: biotin-MCL complex; MM/GBSA, molecular mechanics/generalized Born surface area  
36 continuum salvation; *shPKM2*, specific short hairpin RNA for gene *PKM2*; *shControl*, specific  
37 short hairpin RNA mock; 2dpf, 2 days post fertilization; AAALAC, Assessment and  
38 Accreditation of Laboratory Animal Care; PME, the particle mesh Ewald; MM/GBSA, the  
39 generalized Born and surface area continuum salvation; IPTG, isopropyl  $\beta$ -D-1-  
40 thiogalactopyranoside.  
41  
42  
43  
44  
45  
46  
47  
48  
49  
50  
51  
52  
53  
54  
55  
56  
57  
58  
59  
60

**AUTHOR INFORMATION****Corresponding Authors**

\*Yue Chen: [yuechen@nankai.edu.cn](mailto:yuechen@nankai.edu.cn)

\*Peng G. Wang: [pwang11@gsu.edu](mailto:pwang11@gsu.edu)

**Funding Sources**

This work was supported, in part, by grants from the National Science Fund for Distinguished Young Scholars of China (NO. 81625021), the National Institutes of Health (U01GM116263), National Institutes of Health (GM110387), the Natural Science Foundation of China (NO. 31000371), the International Science & Technology Cooperation Program of China (NO. 2015DFR40460), the Natural Science Foundation of Tianjin (15JCYBJC29000). Computational resources were provided in part by a National Science Foundation XSEDE allocation (CHE110042) and by the National Energy Research Scientific Computing Center (NERSC) supported by the U.S. Department of Energy Office of Science (DE-AC02-05CH11231).

**Notes**

The authors declare no competing financial interest.

**ACKNOWLEDGEMENT**

We thank Qunying Lei of for kindly provided antibody for K433 acetylation of PKM2. We also thank Jenny Yang, Zhiren Liu and Binghe Wang of Georgia State University for their help in instruction of experiments.

**REFERENCES**

- 1  
2  
3  
4  
5  
6 1. Christofk, H. R.; Vander Heiden, M. G.; Harris, M. H.; Ramanathan, A.; Gerszten, R. E.; Wei,  
7  
8 R.; Fleming, M. D.; Schreiber, S. L.; Cantley, L. C. The M2 splice isoform of pyruvate kinase is  
9  
10 important for cancer metabolism and tumour growth. *Nature* **2008**, *452*, 230-233.
- 11  
12 2. Chaneton, B.; Hillmann, P.; Zheng, L.; Martin, A. C.; Maddocks, O. D.; Chokkathukalam, A.;  
13  
14 Coyle, J. E.; Jankevics, A.; Holding, F. P.; Vousden, K. H.; Frezza, C.; O'Reilly, M.; Gottlieb, E.  
15  
16 Serine is a natural ligand and allosteric activator of pyruvate kinase M2. *Nature* **2012**, *491*, 458-  
17  
18 462.
- 19  
20 3. Dayton, T. L.; Jacks, T.; Vander Heiden, M. G. PKM2, cancer metabolism, and the road ahead.  
21  
22  
23 *EMBO Rep* **2016**, *17*, 1721-1730.
- 24  
25 4. Keller, K. E.; Tan, I. S.; Lee, Y. S. SAICAR stimulates pyruvate kinase isoform M2 and  
26  
27 promotes cancer cell survival in glucose-limited conditions. *Science* **2012**, *338*, 1069-1072.
- 28  
29 5. Israelsen, W. J.; Dayton, T. L.; Davidson, S. M.; Fiske, B. P.; Hosios, A. M.; Bellinger, G.; Li,  
30  
31 J.; Yu, Y.; Sasaki, M.; Horner, J. W.; Burga, L. N.; Xie, J.; Jurczak, M. J.; DePinho, R. A.; Clish,  
32  
33 C. B.; Jacks, T.; Kibbey, R. G.; Wulf, G. M.; Di Vizio, D.; Mills, G. B.; Cantley, L. C.; Vander  
34  
35 Heiden, M. G. PKM2 isoform-specific deletion reveals a differential requirement for pyruvate  
36  
37 kinase in tumor cells. *Cell* **2013**, *155*, 397-409.
- 38  
39 6. Azoitei, N.; Becher, A.; Steinestel, K.; Rouhi, A.; Diepold, K.; Genze, F.; Simmet, T.;  
40  
41 Seufferlein, T. PKM2 promotes tumor angiogenesis by regulating HIF-1alpha through NF-  
42  
43 kappaB activation. *Mol Cancer* **2016**, *15*, 3-3.
- 44  
45 7. Gao, X.; Wang, H.; Yang, J. J.; Liu, X.; Liu, Z. R. Pyruvate kinase M2 regulates gene  
46  
47 transcription by acting as a protein kinase. *Mol Cell* **2012**, *45*, 598-609.
- 48  
49  
50  
51  
52  
53  
54  
55  
56  
57  
58  
59  
60

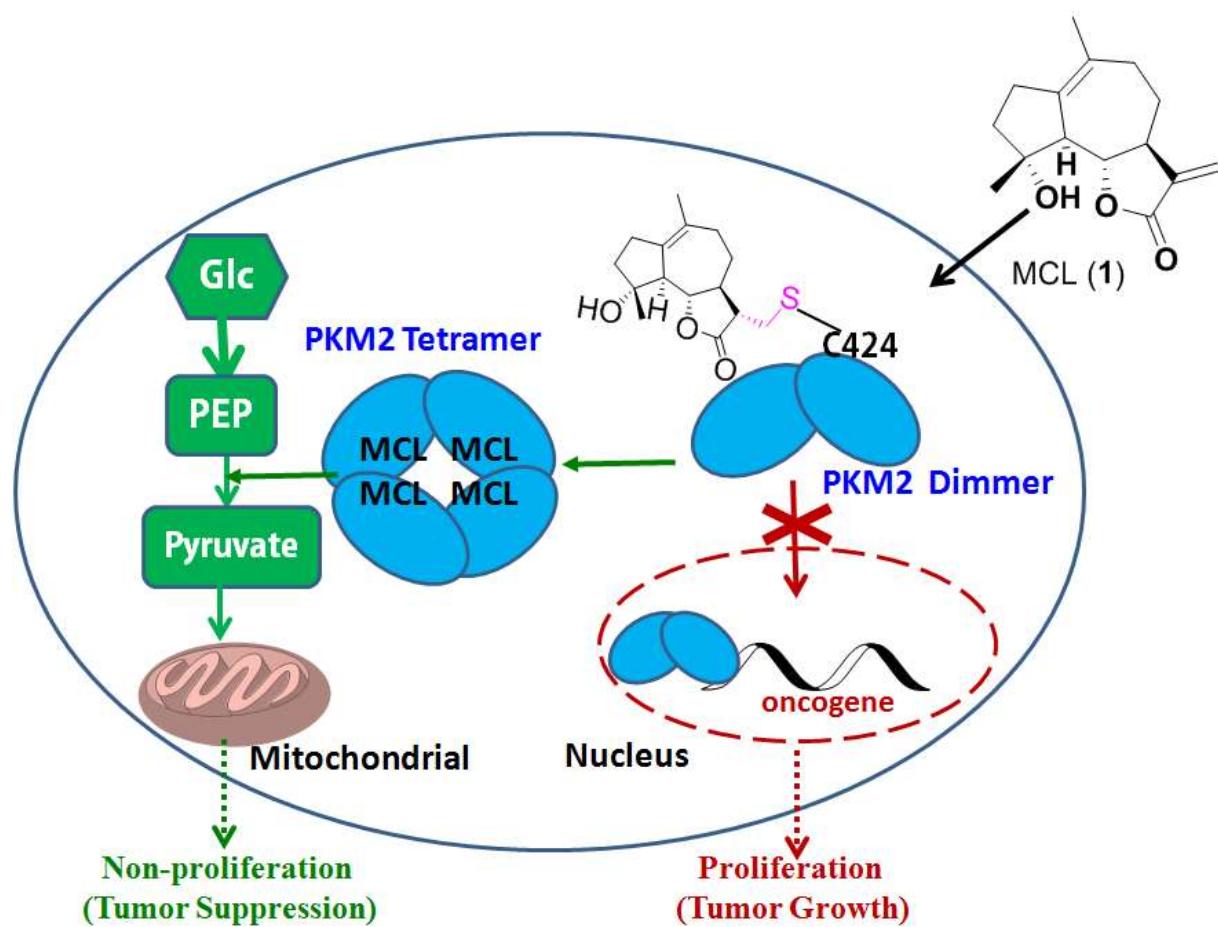
- 1  
2  
3  
4  
5  
6 8. Yang, W.; Xia, Y.; Hawke, D.; Li, X.; Liang, J.; Xing, D.; Aldape, K.; Hunter, T.; Alfred  
7  
8 Yung, W. K.; Lu, Z. PKM2 phosphorylates histone H3 and promotes gene transcription and  
9  
10 tumorigenesis. *Cell* **2012**, *150*, 685-696.  
11  
12  
13 9. Anastasiou, D.; Yu, Y.; Israelsen, W. J.; Jiang, J. K.; Boxer, M. B.; Hong, B. S.; Tempel, W.;  
14  
15 Dimov, S.; Shen, M.; Jha, A.; Yang, H.; Mattaini, K. R.; Metallo, C. M.; Fiske, B. P.; Courtney,  
16  
17 K. D.; Malstrom, S.; Khan, T. M.; Kung, C.; Skoumbourdis, A. P.; Veith, H.; Southall, N.;  
18  
19 Walsh, M. J.; Brimacombe, K. R.; Leister, W.; Lunt, S. Y.; Johnson, Z. R.; Yen, K. E.; Kunii, K.;  
20  
21 Davidson, S. M.; Christofk, H. R.; Austin, C. P.; Inglese, J.; Harris, M. H.; Asara, J. M.;  
22  
23 Stephanopoulos, G.; Salituro, F. G.; Jin, S.; Dang, L.; Auld, D. S.; Park, H. W.; Cantley, L. C.;  
24  
25 Thomas, C. J.; Vander Heiden, M. G. Pyruvate kinase M2 activators promote tetramer formation  
26  
27 and suppress tumorigenesis. *Nat Chem Biol* **2012**, *8*, 839-847.  
28  
29  
30 10. DeLaBarre, B.; Hurov, J.; Cianchetta, G.; Murray, S.; Dang, L. Action at a distance: allostery  
31  
32 and the development of drugs to target cancer cell metabolism. *Chem Biol* **2014**, *21*, 1143-1161.  
33  
34  
35 11. Mann, J. Natural products in cancer chemotherapy: past, present and future. *Nat Rev Cancer*  
36  
37 **2002**, *2*, 143-148.  
38  
39  
40 12. Guzman, M. L.; Rossi, R. M.; Karnischky, L.; Li, X.; Peterson, D. R.; Howard, D. S.; Jordan,  
41  
42 C. T. The sesquiterpene lactone parthenolide induces apoptosis of human acute myelogenous  
43  
44 leukemia stem and progenitor cells. *Blood* **2005**, *105*, 4163-4169.  
45  
46  
47 13. Wiedhopf, R. M.; Young, M.; Bianchi, E.; Cole, J. R. Tumor inhibitory agent from *Magnolia*  
48  
49 *grandiflora* (Magnoliaceae). I. Parthenolide. *J Pharm Sci* **1973**, *62*, 345-345.  
50  
51  
52 14. Jin, P.; Madieh, S.; Augsburger, L. L. The solution and solid state stability and excipient  
53  
54 compatibility of parthenolide in feverfew. *AAPS PharmSciTech* **2007**, *8*, E105.  
55  
56  
57  
58  
59  
60

- 1  
2  
3  
4  
5  
6 15. An, Y.; Guo, W.; Li, L.; Xu, C.; Yang, D.; Wang, S.; Lu, Y.; Zhang, Q.; Zhai, J.; Fan, H.;  
7  
8 Qiu, C.; Qi, J.; Chen, Y.; Yuan, S. Micheliolide derivative DMAMCL inhibits glioma cell  
9  
10 growth *in vitro* and *in vivo*. *PLoS One* **2015**, *10*, e0116202.  
11  
12  
13 16. Zhang, Q.; Lu, Y.; Ding, Y.; Zhai, J.; Ji, Q.; Ma, W.; Yang, M.; Fan, H.; Long, J.; Tong, Z.  
14  
15 Guaianolide sesquiterpene lactones, a source to discover agents that selectively inhibit acute  
16  
17 myelogenous leukemia stem and progenitor cells. *Journal of medicinal chemistry* **2012**, *55*,  
18  
19 8757-8769.  
20  
21  
22 17. Anastasiou, D.; Poulogiannis, G.; Asara, J. M.; Boxer, M. B.; Jiang, J. K.; Shen, M.;  
23  
24 Bellinger, G.; Sasaki, A. T.; Locasale, J. W.; Auld, D. S.; Thomas, C. J.; Vander Heiden, M. G.;  
25  
26 Cantley, L. C. Inhibition of pyruvate kinase M2 by reactive oxygen species contributes to  
27  
28 cellular antioxidant responses. *Science* **2011**, *334*, 1278-1283.  
29  
30  
31 18. Ahn, K.; Johnson, D. S.; Mileni, M.; Beidler, D.; Long, J. Z.; McKinney, M. K.; Weerapana,  
32  
33 E.; Sadagopan, N.; Liimatta, M.; Smith, S. E.; Lazerwith, S.; Stiff, C.; Kamtekar, S.;  
34  
35 Bhattacharya, K.; Zhang, Y.; Swaney, S.; Van Becelaere, K.; Stevens, R. C.; Cravatt, B. F.  
36  
37 Discovery and characterization of a highly selective FAAH inhibitor that reduces inflammatory  
38  
39 pain. *Chem Biol* **2009**, *16*, 411-420.  
40  
41  
42 19. Christofk, H. R.; Vander Heiden, M. G.; Wu, N.; Asara, J. M.; Cantley, L. C. Pyruvate kinase  
43  
44 M2 is a phosphotyrosine-binding protein. *Nature* **2008**, *452*, 181-186.  
45  
46  
47 20. Lv, L.; Xu, Y. P.; Zhao, D.; Li, F. L.; Wang, W.; Sasaki, N.; Jiang, Y.; Zhou, X.; Li, T. T.;  
48  
49 Guan, K. L.; Lei, Q. Y.; Xiong, Y. Mitogenic and oncogenic stimulation of K433 acetylation  
50  
51 promotes PKM2 protein kinase activity and nuclear localization. *Mol Cell* **2013**, *52*, 340-352.  
52  
53  
54  
55  
56  
57  
58  
59  
60

- 1  
2  
3  
4  
5  
6 21. Yang, W.; Xia, Y.; Ji, H.; Zheng, Y.; Liang, J.; Huang, W.; Gao, X.; Aldape, K.; Lu, Z.  
7  
8 Nuclear PKM2 regulates beta-catenin transactivation upon EGFR activation. *Nature* **2011**, *480*,  
9  
10 118-122.  
11  
12 22. Jones, G.; Willett, P.; Glen, R. C.; Leach, A. R.; Taylor, R. Development and validation of a  
13  
14 genetic algorithm for flexible docking. *J Mol Biol* **1997**, *267*, 727-748.  
15  
16 23. Goldberg, M. S.; Sharp, P. A. Pyruvate kinase M2-specific siRNA induces apoptosis and  
17  
18 tumor regression. *J Exp Med* **2012**, *209*, 217-224.  
19  
20 24. Guzman, M. L. Cytokine induced nuclear localization of pyruvate kinase M2 in acute  
21  
22 myeloid leukemia. *Blood* **2013**, *122*, 5406-5406.  
23  
24 25. Hulleman, E.; Broekhuis, M. J.; Pieters, R.; Den Boer, M. L. Pyruvate kinase M2 and  
26  
27 prednisolone resistance in acute lymphoblastic leukemia. *Haematologica* **2009**, *94*, 1322-1324.  
28  
29 26. Wang, Y. H.; Israelsen, W. J.; Lee, D.; Yu, V. W.; Jeanson, N. T.; Clish, C. B.; Cantley, L.  
30  
31 C.; Vander Heiden, M. G.; Scadden, D. T. Cell-state-specific metabolic dependency in  
32  
33 hematopoiesis and leukemogenesis. *Cell* **2014**, *158*, 1309-1323.  
34  
35 27. Cortés-Cros, M.; Hemmerlin, C.; Ferretti, S.; Zhang, J.; Gounarides, J. S.; Yin, H.; Muller,  
36  
37 A.; Haberkorn, A.; Chene, P.; Sellers, W. R. M2 isoform of pyruvate kinase is dispensable for  
38  
39 tumor maintenance and growth. *Proc Natl Acad Sci U S A* **2013**, *110*, 489-494.  
40  
41 28. Wang, Y.; Liu, J.; Jin, X.; Zhang, D.; Li, D.; Hao, F.; Feng, Y.; Gu, S.; Meng, F.; Tian, M.;  
42  
43 Zheng, Y.; Xin, L.; Zhang, X.; Han, X.; Aravind, L.; Wei, M. O-GlcNAcylation destabilizes the  
44  
45 active tetrameric PKM2 to promote the Warburg effect. *Proc Natl Acad Sci U S A* **2017**, *114*,  
46  
47 13732-13737.  
48  
49  
50  
51  
52  
53  
54  
55  
56  
57  
58  
59  
60

- 1  
2  
3  
4  
5  
6 29. Liu, F.; Ma, F.; Wang, Y.; Hao, L.; Zeng, H.; Jia, C.; Wang, Y.; Liu, P.; Ong, I. M.; Li, B.;  
7  
8 Chen, G.; Jiang, J.; Gong, S.; Li, L.; Xu, W. PKM2 methylation by CARM1 activates aerobic  
9  
10 glycolysis to promote tumorigenesis. *Nat Cell Biol* **2017**, *19*, 1358-1370.  
11  
12 30. Jiang, Y.; Wang, Y.; Wang, T.; Hawke, D. H.; Zheng, Y.; Li, X.; Zhou, Q.; Majumder, S.; Bi,  
13  
14 E.; Liu, D. X.; Huang, S.; Lu, Z. PKM2 phosphorylates MLC2 and regulates cytokinesis of  
15  
16 tumour cells. *Nat Commun* **2014**, *5*, 5566-5566.  
17  
18 31. Luo, W.; Hu, H.; Chang, R.; Zhong, J.; Knabel, M.; O'Meally, R.; Cole, R. N.; Pandey, A.;  
19  
20 Semenza, G. L. Pyruvate kinase M2 is a PHD3-stimulated coactivator for hypoxia-inducible  
21  
22 factor 1. *Cell* **2011**, *145*, 732-744.  
23  
24 32. Parnell, K. M.; Foulks, J. M.; Nix, R. N.; Clifford, A.; Bullough, J.; Luo, B.; Senina, A.;  
25  
26 Vollmer, D.; Liu, J.; McCarthy, V.; Xu, Y.; Saunders, M.; Liu, X. H.; Pearce, S.; Wright, K.;  
27  
28 O'Reilly, M.; McCullar, M. V.; Ho, K. K.; Kanner, S. B. Pharmacologic activation of PKM2  
29  
30 slows lung tumor xenograft growth. *Mol Cancer Ther* **2013**, *12*, 1453-1460.  
31  
32  
33  
34  
35  
36  
37  
38  
39  
40  
41  
42  
43  
44  
45  
46  
47  
48  
49  
50  
51  
52  
53  
54  
55  
56  
57  
58  
59  
60

## TOC



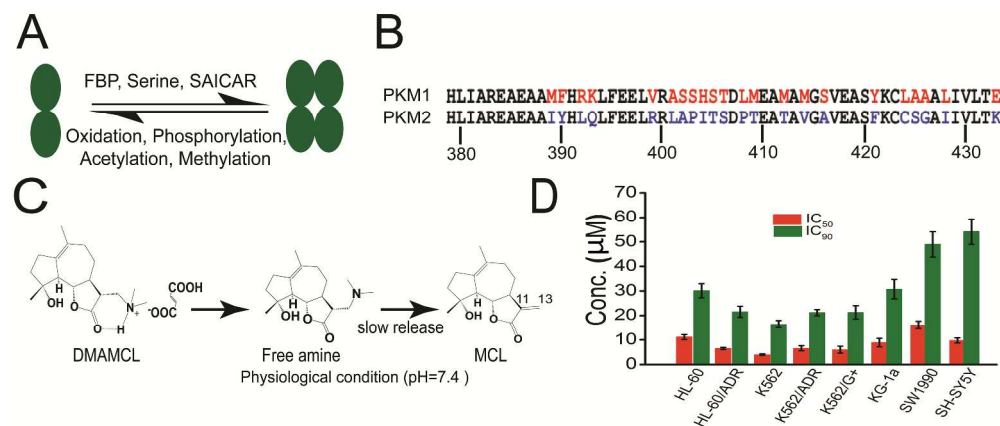


Figure 1. MCL is a novel allosteric activator of PKM2. (A), Allosteric regulations of PKM2. (B), Splice variant amino acids between PKM1 and PKM2. The 22 distinct amino acids are marked in red for PKM1 and in blue for PKM2. (C), the mechanism of sustainable release of MCL by DMAMCL under neutral conditions. (D), Inhibition profile of cancer cell lines by DMAMCL. Eight cancer cell lines were incubated with different concentrations of DMAMCL for 48 h. Cell proliferation was determined by MTT assay. Graphs depict mean  $\pm$  SEM from 6 independent experiments.

1403x595mm (72 x 72 DPI)

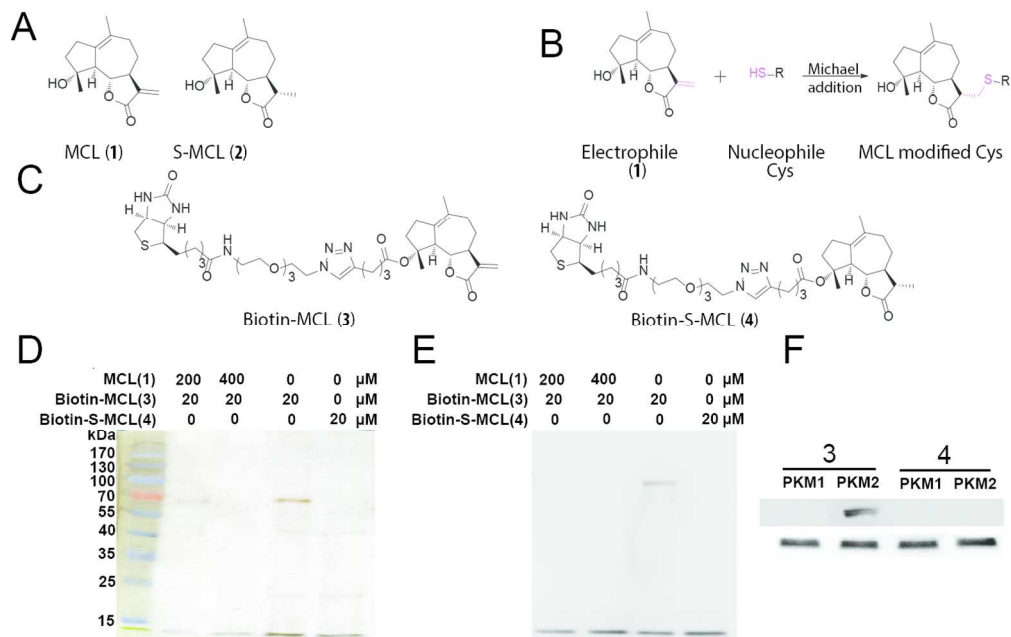


Figure 2. MCL directly binds to PKM2. (A), Structures of MCL (1, active) and S-MCL (2, inactive). (B), Michael addition mechanism of MCL and cysteine. (C), Structure of Biotin-MCL (3, active) and Biotin-S-MCL (4, inactive). (D), Silver staining of the pull-down fraction. HL60 cell lysates were incubated with 3 and 4 at 4°C overnight. For the treatment of 3, a high concentration of MCL was added to the co-incubation. The lysates were used for streptavidin-agarose pull-down assays, and the precipitates were resolved by SDS-PAGE, followed by silver staining. (E), Western blot with the same sample as in silver staining but developed by anti-PKM2. (F), Western blot detection of the binding abilities of 3 and 4 with recombinant proteins PKM1 and PKM2, respectively. rPKM1 and rPKM2 were incubated with probe 3 or 4 at 4°C overnight. The mixture was then subjected to Western blot with streptavidin-HRP to detect the biotin-conjugated complex (top). The same sample was developed with anti-PKM1/PKM2 antibody (bottom) to show the sample amount. All experiments were repeated at least three times, with similar results.

546x346mm (72 x 72 DPI)

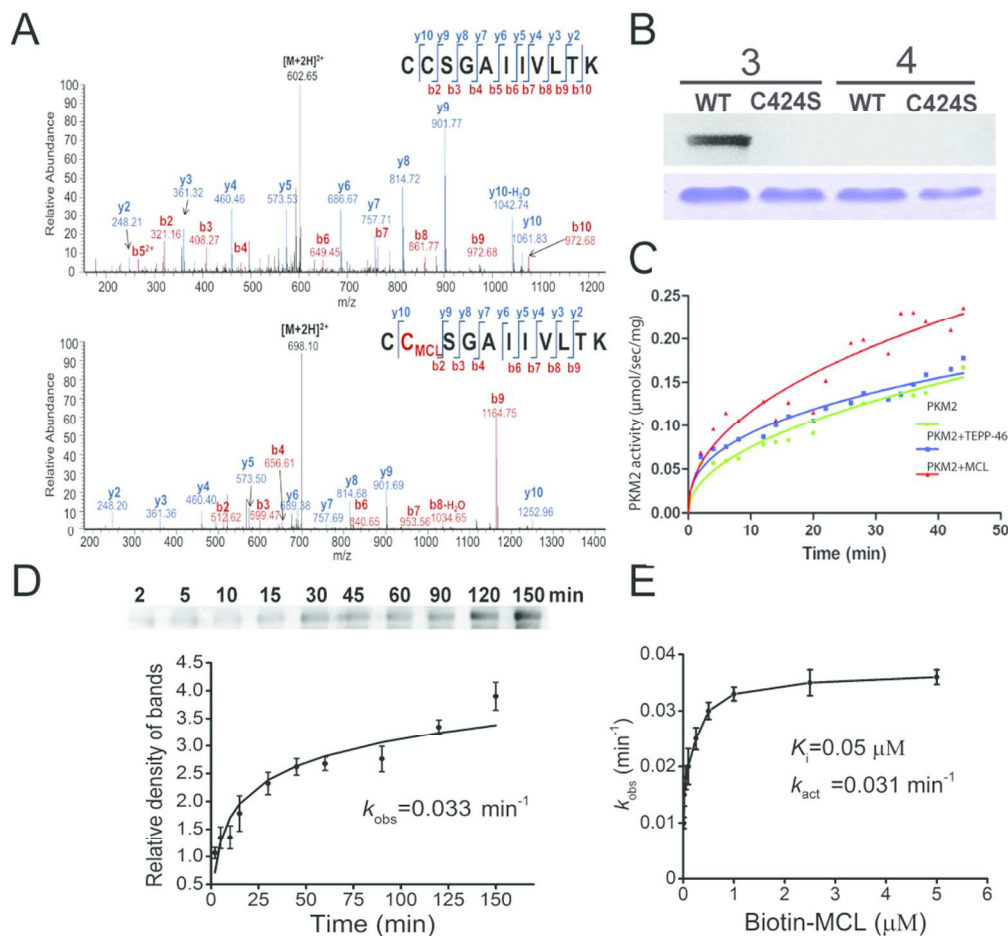


Figure 3. MCL targets C424 of PKM2 and activates its pyruvate kinase activity. (A), MS/MS analysis of the C424-containing tryptic peptide for rPKM2 incubated without (top) and with (bottom) MCL for 60 min at RT. C in red color represents the cysteine bound by MCL. (B), Recombinant WT PKM2 and its mutant (C424S) incubated with biotin-MCL for 60 min at RT, followed by SDS-PAGE (top) and Western blot to detect biotin (top) and PKM2 (bottom). (C), Recombinant PKM2 proteins were incubated with MCL, TEPP-46 at 4  $\mu\text{M}$  for 50 min at RT, and their pyruvate kinase activity was monitored over 40 min. (D), Determination of  $K_{obs}$  for the interaction of PKM2 (0.25  $\mu\text{M}$ ) with biotin-MCL (20  $\mu\text{M}$ ) for different periods of time, as described in the Supplementary Methods. (E), Plotting the  $K_{obs}$  values for the binding of PKM2 as a function of MCL at different concentrations.

389x363mm (72 x 72 DPI)

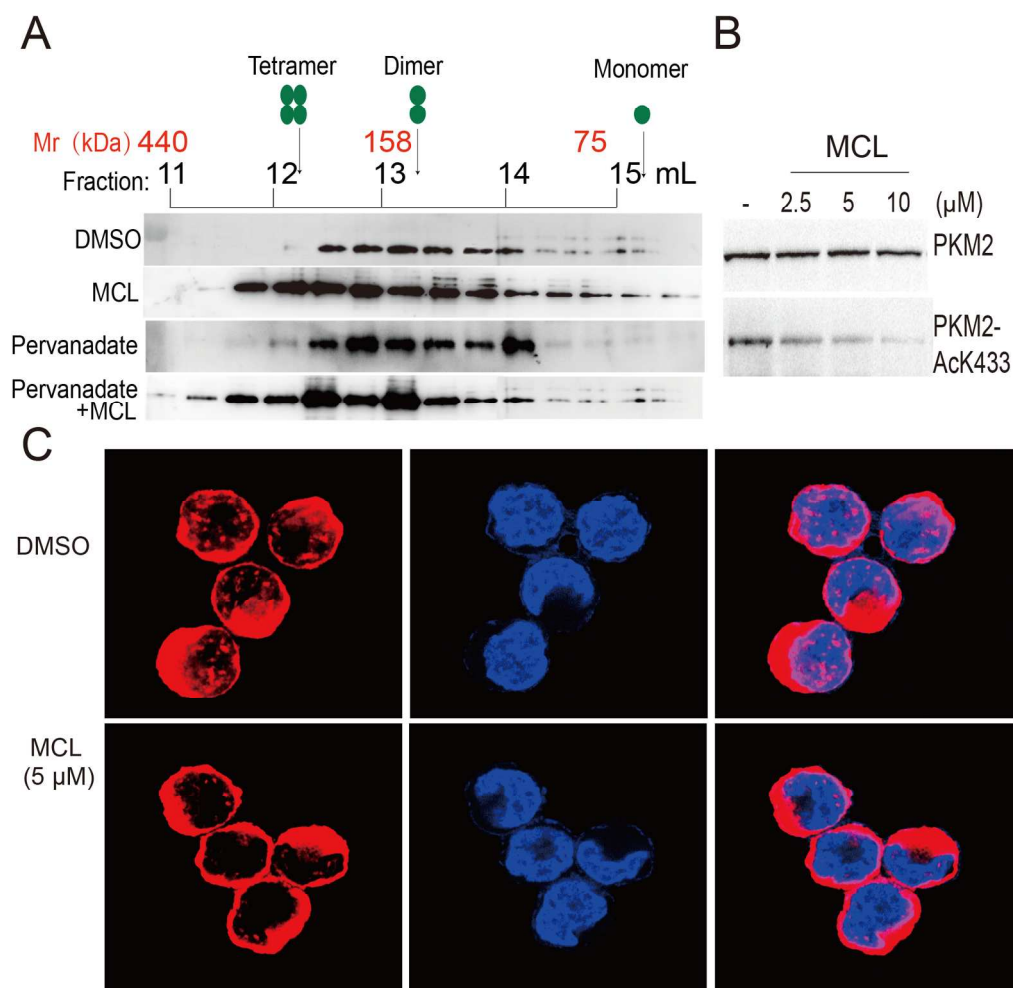


Figure 4. MCL promotes PKM2 tetramer formation and prevents AcK433 modification and nucleus translocation. (A), PKM2 subunit association was determined by western blot using anti-PKM2 (Cell signaling technology, 4053) of the chromatographic fractions of HL60 cells treated with MCL, pervanadate, and MCL combined pervanadate, lysed hypotonically and analyzed by size-exclusion chromatography. Mr, relative molecular weight. (B), Effect of MCL on the AcK433 of PKM2. HL60 cells were preincubated with MCL (0, 2.5, 5 and 10 μM) for 20h, followed by detection of endogenous PKM2 and AcK433 PKM2 by western blot. (C), Subcellular localization of total PKM2 and MCL treated PKM2 was examined by immunofluorescence microscopy in HL60 cells. HL60 cells were treated with MCL (5 μM) or DMSO for 20 h and reacted with anti-PKM2. After overnight incubation, the second antibody Alexa Fluor 647 conjugated goat anti-rabbit IgG (red) for PKM2 and Hoechst 33342 (blue) for nucleus were added to image.

705x693mm (72 x 72 DPI)

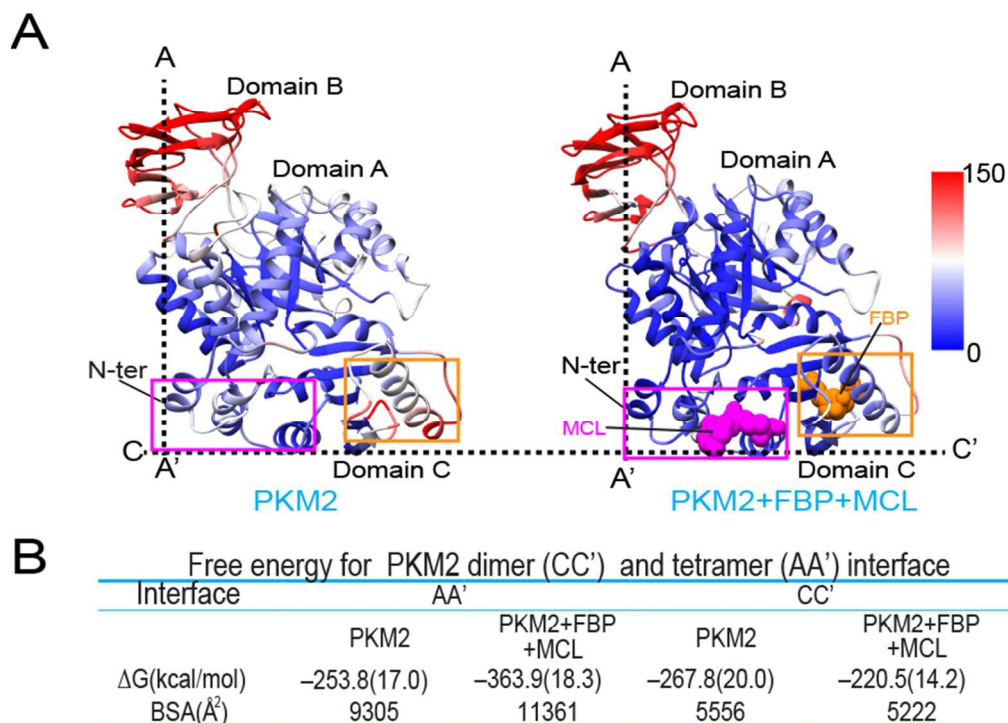


Figure 5. Activator MCL promotes PKM2 tetramer formation (PDB ID: 1ZJH and 1T5A, 1ZJH is the apo tetrameric PKM2 structure. 1T5A is the FBP bound tetrameric PKM2 structure). (A), Computed B-factors mapped onto the PKM2 models highlights conformational differences. Coloring corresponds to computed B-factor values from high (red) to low (blue). (B), Computed free energy of AA' and CC' interface. Per residue binding energies computed from the 1D MM/GBSA decomposition. Residues are colored according to the value of the binding energy in kcal/mol from red (positive) to blue (negative). The bound MCL are shown as magenta spheres. The large (AA') and small (CC') interfaces between monomers are presented as dashed lines. Only one monomer is shown.

315x227mm (72 x 72 DPI)

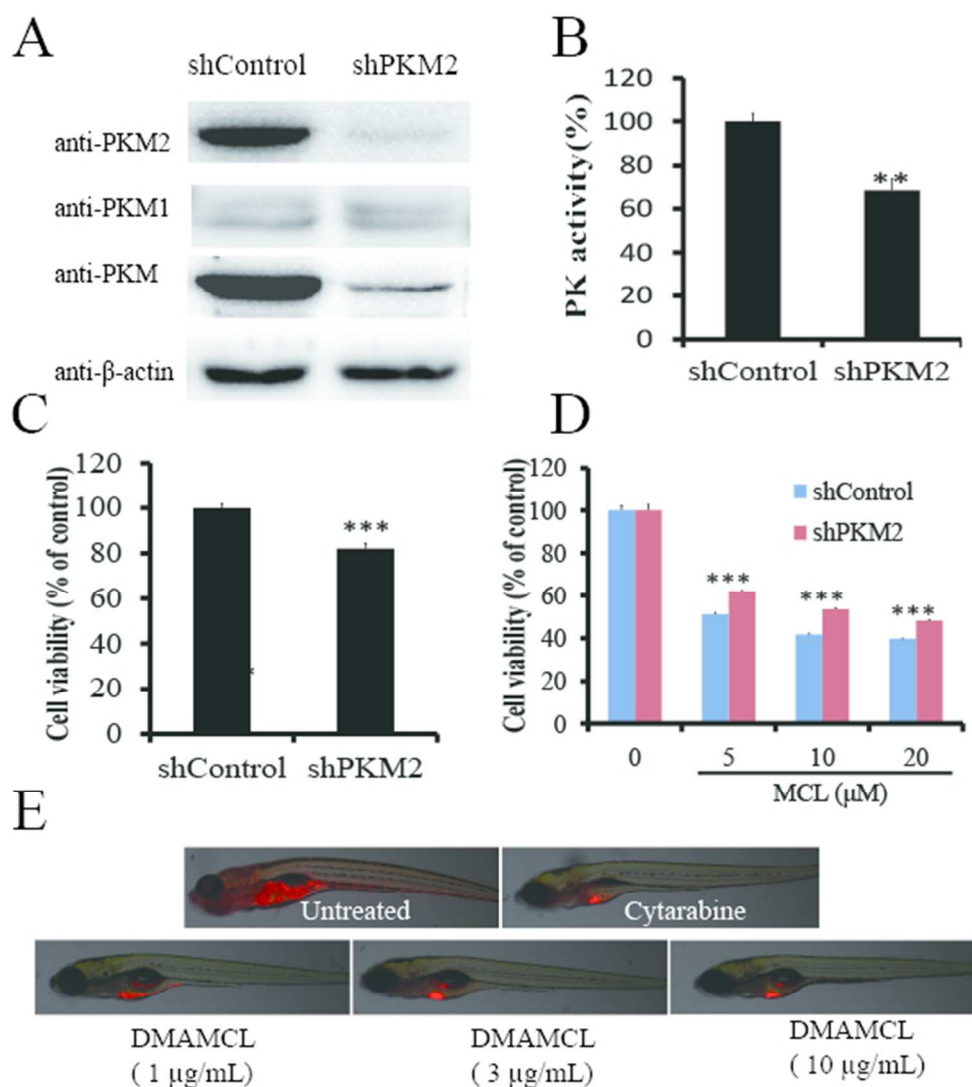


Figure 6. The anticancer effects of DMAMCL are dependent on PKM2. (A), Western blot detection of the expression of PKM1, PKM2 and PKM in the absence of endogenous PKM2, which was knocked down with short hairpin RNA. (B), Cell-based detection of pyruvate activity of HL60 cells with shPKM2 and shControl. (C), Cell viability detection of pyruvate activity of HL60 cells with shPKM2 and shControl. (D), PKM2 depletion desensitizes cancer cells to MCL treatment. (E), Representative fluorescent images of HL60 cell xenografted zebrafishes with treatment of DMAMCL, cytarabine or negative control. Approximately 300 HL60 cells were injected into the yolk sac of embryos. After injections, xenografted embryos were treated with a series of doses of DMAMCL (1, 3, 10 μg/mL), cytarabine at 200 μg/mL as a positive drug control, and saline as a negative control. After 3 days incubation, the number of embryos exhibiting cancer cell dissemination was counted by microscopic observation (15 larvae / group). Data represent the average ± SD of three independent assays. \* =  $P < 0.05$ . \*\* =  $P < 0.01$ .

216x237mm (72 x 72 DPI)

